in *p*-methoxyphenol, so that it cannot serve as a donor in hydrogen bonding to solvent water, these effects are not observed. Thus, conversion of anisole to *p*-methoxyphenol enhances its water affinity by 5.5 orders of magnitude, even more than expected from the benzene–phenol comparison.

The possibility that solvation of benzoquinone may also be "anticooperative" is clouded by the absence of closely related model compounds for comparison. However, *p*-benzoquinone, with two carbonyl groups, is only 3.7 orders of magnitude more hydrophilic than benzene, whereas acetone, with only a single carbonyl group, is 4.4 orders of magnitude more hydrophilic than propane. This apparent lack of hydrophilic character in *p*-benzoquinone, compared with benzene, may also be related, at least in part, to the absence of aromatic character that might render the π electrons of benzene accessible to hydrogen bonding interactions with solvent water.

p-Benzoquinone is about 3.2 orders of magnitude less strongly solvated by water than is *p*-hydroquinone. Because hydroquinone is so much more strongly solvated than benzoquinone, its reducing power in water is less by approximately 4.3 kcal (0.2 V) than it would be in surroundings of unit dielectric constant. Unless other biological redox pairs are affected to the same extent by removal from solvent water, this is a factor that is likely to affect the relative energies of components of the electron transport chain embedded in the mitochondiral inner membrane, as compared with the values that would be observed in dilute aqueous solution.

Registry No. Imidazole, 288-32-4; 1-methylimidazole, 616-47-7; 4-methylimidazole, 822-36-6; pyrrole, 109-97-7; 1-methylpyrrole, 96-54-8; cyclopentadiene, 542-92-7; *o*-nitrophenol, 88-75-5; *m*-nitrophenol, 554-84-7; *p*-nitrophenol, 100-02-7; *p*-benzoquinone, 106-51-4; *p*-hydroquinone, 123-31-9; *p*-methoxyphenol, 150-76-5; benzene, 71-43-2; phenol, 108-95-2; anisole, 100-66-3; nitrobenzene, 98-95-3; picrate/Me_4N^+, 733-60-8; picrate/Et_4N^+, 741-03-7; thiopicrate/Me_4N^+, 105598-14-9; thiopicrate/Et_4N^+, 105598-15-0; 5-nitrosalicylate/Et_4N^+, 105598-16-1; 3,5-dinitrosalicylate/Et_4N^+, 105598-17-2.

Barbituric Acids as Carbon Acids. Acidity Relationships and ^1H and ^2H Transfer in 1,3-Dimethyl-5-*tert*-butyl- and 5-*tert*-Butylbarbituric Acids[1]

D. A. Buckingham,* C. R. Clark, R. H. McKeown, and O. Wong

Contribution from the Departments of Chemistry and Pharmacy, University of Otago, Dunedin, New Zealand. *Received July 16, 1986*

Abstract: Slow ionization and reprotonation at the C_5 carbon atom has been observed for 1,3-dimethyl-5-*tert*-butyl- (1,3-Me_2-5-*t*-Bu), 5-*tert*-butyl- (5-*t*-Bu), 1,3-diisopropyl- (1,3-*i*-Pr_2), and 1,5-diisopropyl- (1,5-*i*-Pr_2) barbituric acids (BA) in aqueous solution at 25.0 °C and I = 0.1 mol dm^{-3} (NaCl). For 1,3-Me_2-5-*t*-Bu(BA) (pK = 9.41) deprotonation follows the rate law $k_f = k_1^{H_2O} + k_1^{OH}[OH^-]$ with $k_1^{H_2O}$ = 4.0 × 10^{-4} s^{-1}, k_1^{OH} = 192 dm^3 mol^{-1} s^{-1} and reprotonation the rate law $k_r = k_{-1}^{H_2O} + k_{-1}^{H}[H^+]$ with $k_{-1}^{H_2O}$ = 8.9 × 10^{-3} s^{-1}, k_{-1}^{H} = 1.12 × 10^6 mol^{-1} dm^3 s^{-1} (pH range 6.91–12.89). For the $^2H(C_5)$ derivative the corresponding dedeuteriation rates are $k_1^{H_2O}$ = 7.7 × 10^{-5} s^{-1} (k_H/k_D = 5.2) and k_1^{OH} = 54 mol^{-1} dm^3 s^{-1} (k_H/k_D = 3.5). Deprotonation is catalyzed by general bases (k^B mol^{-1} dm^3 s^{-1}, k_H/k_D), 2,6-lutidine (0.0108, 10.0), dabco (29.6, 5.5), NH_3 (1.06, 7.1), $EtNH_2$ (14.7, 5.8), Et_2NH (18.0, 7.2), Et_3N (1.30, 7.2), but a linear correlation with pK_{BH} is not observed, and structural effects appear to play an important role. The measurement of precise primary kinetic isotope ratios (k_H/k_D) in water is discussed. In 5-*t*-Bu(BA) (KH_3) ionization at C_5 (pK = 8.09 ± 0.12) to produce the enolate anion (EH_2^-) comes into competition with ionization at imide nitrogen (pK = 7.88 ± 0.04) to produce the keto monoanion (KH_2^-). In strongly alkaline solution the species deprotonated at both imide nitrogen centers (KH^{2-}) is preferred by about 20:1 over the enolate dianion (EH^{2-}) (C_5, and imide nitrogen deprotonated). Such ionizations complicate a study of proton exchange at C_5 but this has been clarified by use of the $^2H(C_5)$ substituted acid (KDH_2). Deprotonation at C_5 occurs via pH independent ($k_1^{H_2O}$ = 2.59 × 10^{-3} s^{-1}, k_H/k_D = 7.1) and OH^- dependent (k_1^{OH} = 800 mol^{-1} dm^3 s^{-1}, k_H/k_D = 3.4) reactions of KH_3 and via the OH^- dependent reaction of KH_2^- (k_2^{OH} = 0.54 mol^{-1} dm^3 s^{-1}). Correspondingly, pathways for reprotonation of the enolate anions are available through the H^+ dependent (k_{-1}^{H} = 3.2 × 10^5 mol^{-1} dm^3 s^{-1}) and pH independent ($k_{-1}^{H_2O}$ = 1.62 × 10^{-3} s^{-1}) reactions of EH_2^- and through the pH independent reaction of EH^{2-} ($k_{-2}^{H_2O} \approx 0.4$ s^{-1}). The known rates of C_5 deprotonation ($k_1^{H_2O}$) and reprotonation (k_{-1}^{H}) for barbituric acids have been correlated with carbon acidity (K_c) via linear Brønsted relationships of slope 0.80 and 0.20, respectively (pK_c range 2.2–9.6). Barbituric acid carbon acidity is thus demonstrated to be controlled largely by substituent effects on the deprotonation reaction.

Two proton transfer studies on barbituric acids have been reported previously. The original classic experiments of Eigen, Ilgenfritz, and Kruse[2] used T-jump to investigate barbituric acid (BA) itself, and Koffer[3] extended this via P-jump and conductimetric detection to the C_5-substituted H, Me, Et, *i*-Pr, and Ph derivatives. These investigations showed that the rate of proton abstraction ($k_1^{H_2O}$), eq 1, varied from 1.33 s^{-1} for R = *i*-Pr to 184

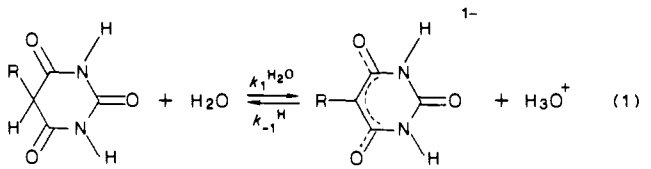

(1)

s^{-1} for *R* = Ph.[3] Reprotonation rates (k_{-1}^{H}) were, however, more constant at ~10^6 dm^3 mol^{-1} s^{-1} for all substrates irrespective of

(1) Abstracted in part from the Ph.D. Dissertation of Wong, O., University of Otago, 1984 (present address IPRX, University of Kansas Research Program; Lawrence, KS). A preliminary account has been given in J. *Chem. Soc., Chem. Commun.* **1984**, 1440.
(2) Eigen, M.; Ilgenfritz, G.; Kruse, W. *Chem. Ber.* **1965**, *98*, 1623.
(3) Koffer, H. *J. Chem. Soc., Perkin Trans. 2* **1975**, 819.

0002-7863/87/1509-0466$01.50/0

their acidity, and the major early interest lay in the relative slowness of reprotonation compared to the classic diffusion controlled processes found for nitrogen and oxygen acids.

When alkali is added to an aqueous solution of 5-*tert*-butyl barbituric acid (5-*t*-Bu(BA)) a slow (s to min), reversible, change occurs in its UV spectrum. Preliminary experiments showed this to result from proton abstraction from C_5 by OH^-, but the slowness of this process compared to those of the earlier studies seemed unusual, and since one of us[4] has been interested for many years in the acidity of barbituric acids, worthy of further study. Although not essential to their pharmacological action ionization at carbon is thought to influence conformational and biological properties.[5] If the rate of ionization varies widely with the C_5 substituent, then this might be a factor in the ability of a particular barbituric acid to be absorbed and to penetrate active sites in vivo.

This investigation reports a detailed study of equilibria and rates of ionization in 5-*t*-Bu(BA), 1,3-Me_2-5-*t*-Bu(BA), and to a lesser extent 1,3-*i*-Pr_2(BA) and 1,5-*i*-Pr_2(BA) and relates the acidity of this class of carbon acid in a general way.

Experimental Section

Synthetic procedures were essentially the same as those given previously.[6,7] Purity of products was checked by thin-layer chromatography with developing solvents chloroform–butanol–ammonium hydroxide (*d* 0.880) (14:8:1) and benzene–methanol–glacial acetic acid (90:16:8). Compounds were detected as follows: (a) mercuric nitrate (0.33% in 0.04 mol dm^{-3} nitric acid) was first sprayed on plates which were dried and then sprayed with diphenylcarbazone (0.1% in 95% ethanol). Acidic species such as barbituric acids and imides appeared as pink or white spots on a blue background; (b) ceric sulfate (5% in 10% sulfuric acid solution) was used to detect organic impurities which appeared as white or brown spots which faded on heating.

Materials. Malonic acid, urea, and 1-isopropylurea were dried under vacuum prior to use. Peroxides in tetrahydrofuran (THF) were removed by treatment with 10% aqueous sodium sulfite solution; the THF was then dried ($MgSO_4$), distilled, and stored over sodium wire. Diisopropyl ether was similarly treated. 2,6-Lutidine and triethylamine were redistilled prior to use. All other reagents were of AR or laboratory reagent grade and were used without further purification.

Deuteration at C_5 in 5-*tert*-butylbarbituric acid and 1,3-dimethyl-5-*tert*-butylbarbituric acid was achieved by dissolving the protic compound (10–20 mg) in CH_3OD (0.5–1.0 cm^3) and adding D_2O (0.2–0.4 cm^3). Exchange in both compounds was complete within 24 h.

5-*tert*-Butylbarbituric Acid. Urea (20 g, 0.30 mol), diethyl *tert*-butylmalonate (67 g, 0.33 mol), and super dry ethanol[9] (150 cm^3) were placed in a 2-L, three-necked flask fitted with a double surface condenser, magnetic stirrer bar, dropping funnel, and thermometer. The flask was placed in a sand bath supported by a combination hot plate–magnetic stirrer. Sodium ethoxide solution[9] in super dry ethanol (21.5 g, 0.93 mol Na, 350 cm^3 EtOH) was added as the mixture was stirred and heated.[6] At about 70 °C a white precipitate appeared and continued to separate as the mixture was refluxed. After 8 h the solid (Na salt of product) was filtered off and dissolved in the minimum volume of ice-cold water. 5-*tert*-Butylbarbituric acid was precipitated by adding hydrochloric acid, filtered off, washed free of acid by using several portions of cold water, and dried under vacuum over silica gel. Recrystallization from water gave a 56% yield of the pure material: mp 240–41 °C (lit.[8] 235.5–236.5 °C); IR $\nu_{C=O}$ 1743, 1708 cm^{-1}; ^1H NMR δ $(CD_3)_2SO$ 1.01 (9 H, s, $(CH_3)_3C$), 2.86 (1 H, s, *H*-C_5), 11.01 (2 H, s, N*H* (exchanged on addition of D_2O)); MS, *m/e* 184 (M). Anal. Calcd for $C_8H_{12}N_2O_3$: C, 52.2; H, 6.6; N, 15.2. Found: C, 52.2; H, 6.5; N, 15.2.

1,3-Dimethyl-5-*tert*-butylbarbituric Acid. 5-*tert*-Butylbarbituric acid (3 g, 0.016 mol), NaOH (1.3 g, 0.032 mol), diisopropyl ether (25 cm^3), and dimethyl sulfate (6.5 g, 0.05 mol) were stirred in water (40 cm^3) at room temperature for 4 h. Workup gave the crude product (3 g, 88%) which was crystallized from water then sublimed under reduced pressure: mp 60–61 °C; $\nu_{C=O}$ 1760, 1700, 1690 cm^{-1}; ^1H NMR δ $(CD_3)_2SO$ 0.87 (9 H, s, $(CH_3)_3C$), 3.08 (1 H, s, *H*-C_5), 3.08 (6 H, s, CH_3-N); MS, *m/e* 212. Anal. Calcd for $C_{10}H_{16}N_2O_3$: C, 56.6; H, 7.6; N, 13.2. Found: C, 56.6; H, 7.8; N, 13.4.

1,5-Diisopropylbarbituric Acid. Diethyl isopropylmalonate[7] (50 g, 0.25 mol), 1-isopropyl urea (32 g, 0.3 mol), and sodium ethoxide (0.32 mol) in ethanol (165 cm^3) were refluxed for 7 h. Following workup recrystallization from water afforded the product (47%): mp 76–77 °C; $\nu_{C=O}$ 1750, 1710, 1690 cm^{-1}; ^1H NMR δ $(CD_3)_2SO$ 0.96 (6 H, d, J = 7 Hz, $(CH_3)_2CH$), 1.31 (6 H, d, J = 7 Hz, $(CH_3)_2CHN$), 2.40 (1 H, m, $(CH_3)_2CH$), 3.18 (1 H, d, J = 4 Hz, *H*C), 4.80 (1 H, sept, J = 7 Hz, $(CH_3)_2CHN$), 11.13 (1 H, s (br), N*H* (exchanged on addition of D_2O)); MS, *m/e* 212. Anal. Calcd for $C_{10}H_{16}N_2O_3$: C, 56.6; H, 7.6; N, 13.2. Found: C, 56.6; H, 7.7; N, 13.2.

1,3-Diisopropylbarbituric Acid. *N,N'*-Diisopropylcarbodiimide (27 g, 0.21 mol) in dry THF (100 cm^3) was added to a cooled solution of malonic acid (10 g, 0.1 mol) in THF (100 cm^3). The reaction mixture was shaken vigorously for 5 min then periodically over a period of 1 h. Precipitated 1,3-diisopropylurea was filtered off; the filtrate was reduced in volume, and water was added. The copious white precipitate was recovered by filtration, and concentration of the aqueous filtrate (rotary evaporator) gave further solid. The combined precipitates (18 g, 88%) were crystallized from water giving 1,3-diisopropylbarbituric acid: mp 131.5–132 °C (lit.[11] mp 128–129 °C); $\nu_{C=O}$ 1700, 1688 cm^{-1}. ^1H NMR δ $(CD_3)_2CO$ 1.35 (12 H, d, J = 7 Hz, $(CH_3)_2CHN$), 3.60 (2 H, s, H_2C), 4.95 (2 H, sept, J = 7 Hz, $(CH_3)_2CHN$); MS, *m/e* 212. Anal. Calcd for $C_{10}H_{16}N_2O_3$: C, 56.6; H, 7.6; N, 13.2. Found: C, 56.4; H, 7.9; N, 13.3.

Kinetics Measurements. Reactions with $t_{1/2} > 10$ s were initiated by addition of a concentrated solution of the barbituric acid in methanol (0.002–0.01 cm^3) to a 1-cm path length cell containing the appropriate buffer or sodium hydroxide solution (3.0 cm^3, 25.0 °C). The cell contents were then rapidly mixed, and absorbance changes were monitored for at least $4t_{1/2}$ at the appropriate wavelength (Cary 219). Faster reactions were carried out by using a Durrum D110 stopped-flow spectrophotometer equipped with a Biomation Model 805 waveform recorder and Tektronix 5110 oscilloscope. Solutions of C_5 deuterated barbituric acids in water were prepared by dilution of CH_3OD/D_2O stock solutions, and exchange reactions were initiated within 3 min of preparation. The exchange reactions and relaxation processes observed for the corresponding protic substrates followed pseudo-first-order kinetics at constant pH and observed rate constants (k_{obsd}) were obtained from plots of log $(A_\infty - A_t)$ or log $(A_t - A_\infty)$ against time. These were linear over at least $3t_{1/2}$.

Apparatus. IR spectra were recorded as KBr discs by use of a Shimadzu IR-400 spectrophotometer. ^1H NMR spectra were obtained by using either Varian T-60 or EM-390 instruments or by use of a JEOL FX-60 spectrometer with tetramethylsilane (TMS) as internal reference. This last instrument was used to obtain ^{13}C NMR spectra. Mass spectra were obtained by use of a Varian CH-7 spectrometer and UV spectra with a Cary 219 instrument. Melting points were determined with an Electrothermal 1A 6304 Mark II melting point apparatus.

pK_a Measurements. pK_a values were determined spectrophotometrically by using standard methods,[12] or by potentiometric titration[6,7] with use of either a Radiometer pHM 26 pH meter equipped with scale expansion or a pHM 62 meter in conjunction with an ABU-12 autoburette and TTT-60 titrator. Except where indicated otherwise all values of equilibrium constants are reported as concentration constants at I = 0.1 mol dm^{-3} (NaCl) with subscripts indicating ionization at carbon (pK_c) or at nitrogen (pK_N) centers. Conversion of these to thermodynamic constants (pK^T) as required was achieved by using a calculated value[13] of 0.776 for the mean molal activity coefficient of a 1:1 electrolyte at this ionic strength.

Results

1. Carbon Acidity in 1,3-Me_2-5-*t*-Bu(BA). In alkaline solution (pH > 11, I = 0.1 mol dm^{-3} (NaCl)) 1,3-Me_2-5-*t*-Bu(BA) exists as the enolate anion (E^-) with λ_{max} = 270 nm ($\epsilon = 1.6 \times 10^4$ mol^{-1} dm^3 cm^{-1}), λ_{max} = 233 nm ($\epsilon = 4.8 \times 10^3$ mol^{-1} dm^3 cm^{-1}). On adding acid to the solution the 270-nm band decreases in intensity (slowly, see below) with a commensurate increase in the 233-nm band, Figure 1 (isosbestic point 239 nm). This change is exactly reversed on titrating an acidic solution of 1,3-Me_2-5-*t*-Bu(BA) with alkali, and the acid form (KH) has λ_{max} = 233 nm ($\epsilon = 7.1 \times 10^3$ mol^{-1} dm^3 cm^{-1}). No further spectral change is observed

(4) McKeown, R. H. Ph.D. *Thesis*, University of Otago, 1976.
(5) Carroll, F. I.; Philip, A.; Moreland, C. G. *J. Med. Chem.* **1976**, *19*, 521.
(6) McKeown, R. H.; Prankerd, R. J. *J. Chem. Soc., Perkin Trans. 2* **1981**, 481.
(7) McKeown, R. H. *J. Chem. Soc., Perkin Trans. 2* **1980**, 504.
(8) Eliel, E. L.; Hutchins, R. O.; Knoeber, S. M. *Org. Synth.* **1970**, *50*, 39.
(9) Vogel, A. I. *A Textbook of Practical Organic Chemistry*, 4th ed.; Longmans: New York, 1978; pp 269, 435.
(10) Bush, M. T. *J. Am. Chem. Soc.* **1939**, *61*, 637.
(11) Bose, A. K.; Garrett, S. *Tetrahedron* **1963**, *19*, 85.
(12) Albert, A.; Serjeant, E. P. *Ionization Constants of Acids and Bases*; Wiley: New York, 1962.
(13) Davies, C. W. *J. Chem. Soc.* **1938**, 2093.

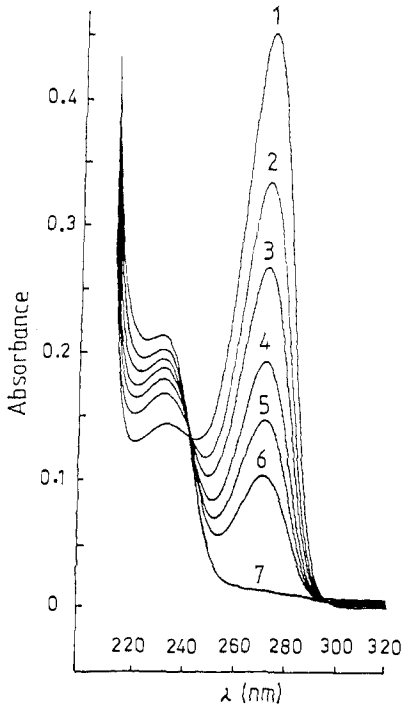

Figure 1. Spectrophotometric titration of 1,3-dimethyl-5-*tert*-butylbarbituric acid (3×10^{-5} mol dm^{-3}, I = 0.1 mol dm^{-3} NaCl) in the presence of 0.02 mol dm^{-3} NH_3 (aqueous) at 25 °C with $HClO_4$. pH's: (1) 10.62; (2) 9.81; (3) 9.56; (4) 9.30; (5) 9.12; (6) 8.90; (7) 4.18.

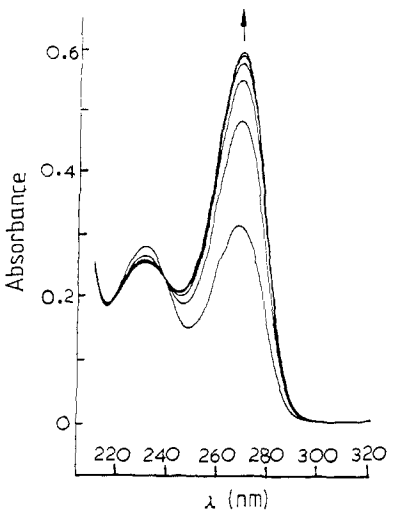

Figure 2. Spectral scans (time interval 22.5 s) following addition of 1,3-dimethyl-5-*tert*-butylbarbituric acid (5.2×10^{-5} mol dm^{-3}) to borax buffer (1.25×10^{-2} mol dm^{-3}, pH 9.8 at 25 °C and I = 0.1 mol dm^{-3} NaCl).

below pH 7 or above pH 11. It is clear that a single acid–base equilibrium is being observed, and analysis of the 270-nm data gives pK_c = 9.41 ± 0.02, 25.0 °C, I = 0.1 mol dm^{-3} (NaCl). This value corresponds to pK_c^T = 9.63 ± 0.02 and is to be compared with the potentiometrically determined thermodynamic value of 9.60 ± 0.01 (Table IX).

2. ^{1}H- and ^{2}H-Transfer in 1,3-Me$_2$-5-*t*-Bu(BA). Figure 2 shows spectral traces taken at 22.5-s intervals after a solution of 1,3-Me$_2$-5-*t*-Bu(BA) initially at pH ~ 5 was rapidly mixed with borate buffer to give a final pH of 9.8; the data at the 270-nm maximum plot as a first-order process with $t_{1/2}$ = 18.0 s. A detailed kinetic analysis of this process was undertaken in the pH range 7–13 at 25.0 °C and I = 0.1 mol dm^{-3} (NaCl) by using buffers to maintain constant pH (at least a 50-fold excess over [BA] ≈ 5×10^{-5} mol dm^{-3}), and an analogous study was carried out on the C_5-deuterated acid. Good pseudo-first-order rate data were obtained over at least 3 half-lives in every case. The processes

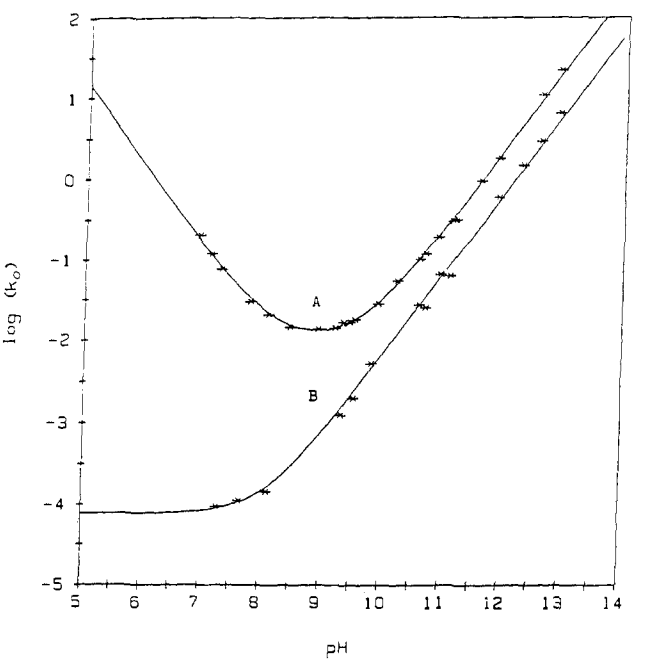

Figure 3. pH-rate profiles for proton transfer (A) and deuterium exchange (B) at C_5 in 1,3-dimethyl-5-*tert*-butylbarbituric acid at 25 °C and I = 0.1 mol dm^{-3} (NaCl). Experimental points are indicated (*) and the curves are calculated from eq 4 and 5, respectively, by using the values of the constants given in the text.

were initiated either by adding a concentrated solution of the barbituric acid in methanol to the appropriate buffer or by mixing equal volumes of buffer with a solution of the barbituric acid in water. The presence of methanol (typically 1–2%) did not affect the observed rates, and for the ^{1}H substrate at a particular pH identical rates were obtained irrespective of the direction from which the equilibrium was approached (upward or downward pH perturbation), or of the magnitude of the pH jump (up to 8 pH units). The processes were significantly catalyzed by the buffer species (see below), and to obtain buffer independent solvolytic rate constants (k_0) it was necessary to obtain k_{obsd} at several buffer concentrations ($[B]_T = [BH^+] + [B]$). Plots of k_{obsd} vs. $[B]_T$ were linear with positive gradients, and the nonzero intercepts gave k_0 values. In many cases, particularly where $[B]_T$ lay in the range $1–5 \times 10^{-2}$ mol dm^{-3}, the contribution to catalysis by the buffer was only 5–20% and this, while allowing k_0 to be well-defined, was insufficient to afford accurate rate constants for buffer catalysis. These were subsequently determined by using higher buffer concentrations (see below).

Rate data are given in Table I (Supplementary Material) and Figure 3 gives plots of log k_0 vs. pH for both the ^{1}H and ^{2}H derivatives. The plot for the former is clearly U-shaped, exhibiting limiting first order in $[H^+]$ dependence for pH < 7 and first order in $[OH^-]$ behavior for pH > 10.5. The rate minimum occurs at pH 8.9. For the ^{2}H reactant k_0 is largely pH independent in the range 7–8 but increases to exhibit a first order in $[OH^-]$ dependence above pH 9.5. The reaction is always slower than that for the ^{1}H derivative.

The pH rate profile for H exchange in the ^{1}H acid fits expression 2

$$k_0 = k + k_1[H^+] + k_2[OH^-] \quad (2)$$

with $k = 9.3 \times 10^{-3}$ s^{-1}, $k_1 = 1.12 \times 10^6$ dm^3 mol^{-1}, s^{-1}, $k_2 = 1.92 \times 10^2$ dm^3 mol^{-1} s^{-1} at 25.0 °C, and I = 0.1 mol dm^{-3} (NaCl). At the minimum of the curve (pH 8.9, Figure 3) the first term (k) accounts for 70% of the rate so that all three contributions are well defined.

Since only KH and E$^-$ are present at equilibrium in the pH range 7–13 (see above) the process given by eq 3 may be treated

$$KH + H_2O/OH^- \underset{k_r}{\overset{k_f}{\rightleftharpoons}} E^- + H_3O^+/H_2O \quad (3)$$

Table II. Rate Constants for ^1H and ^2H Transfer in 1,3-Dimethyl-5-*tert*-butylbarbituric Acid at 25 °C and I = 0.1 mol dm^{-3} (NaCl)

reactant	$k_1^{H_2O}$ (s^{-1})	k_1^{OH} (dm^3 mol^{-1} s^{-1})	k_{-1}^{H} (dm^3 mol^{-1} s^{-1})	$k_{-1}^{H_2O}$ (s^{-1})
C-5 ^1H	4.0×10^{-4}	192	1.12×10^6	8.9×10^{-3}
C-5 ^2H	7.7×10^{-5}	54		
k_H/k_D	5.2	3.5		

as a simple pseudo-first-order relaxation process with $k_0 = k_f + k_r$ and $k_f = k_1^{H_2O} + k_1^{OH}[OH^-]$ and $k_r = k_{-1}^{H}[H^+] + k_{-1}^{H_2O}$ whereby (2) becomes (4)

$$k_0 = k_1^{H_2O} + k_{-1}^{H_2O} + k_{-1}^{H}[H^+] + k_1^{OH}[OH^-] \quad (4)$$

Then $k_1^{H_2O} + k_{-1}^{H_2O} = 9.3 \times 10^{-3}$ s^{-1}, $k_{-1}^{H} = 1.12 \times 10^6$ dm^3 mol^{-1} s^{-1}, and $k_1^{OH} = 192$ dm^3 mol^{-1} s^{-1}. The microscopically related rate constants $k_1^{H_2O}$, $k_{-1}^{H_2O}$ must agree with the equilibrium condition $k_1^{H_2O} = k_{-1}^{H}K_c$, $k_{-1}^{H_2O} = k_1^{OH}K_w/K_c$ ($K_w = [H^+][OH^-] = K_w^T/f_+^2 = 1.00 \times 10^{-14}/(0.776)^2 = 1.66 \times 10^{-14}$ mol^2 dm^{-6}) from which $k_1^{H_2O}$, $k_{-1}^{H_2O}$, and K_c may be obtained. The three independent variables k_{-1}^{H}, k_1^{OH}, and K_c were least squares fitted to the experimental data, and the full curve (Figure 3) was obtained by using the rate constants listed in Table II, and $K_c = 3.58 \times 10^{-10}$ mol dm^{-3} ($pK_c = 9.45$). This latter value is in good agreement with that obtained from the spectrophotometric measurement ($pK_c = 9.41$, see above).

Displacement of ^2H in the C_5-deuterated acid (KD) follows the rate law

$$k_0 = k^{H_2O} + k^{OH}[OH^-] \quad (5)$$

and fitting the observed data gives $k^{H_2O} = 7.7 \times 10^{-5}$ s^{-1} and $k^{OH} = 54$ dm^3 mol^{-1} s^{-1} at 25.0 °C, I = 0.1 mol dm^{-3} (NaCl). Ionization of KD occurs irreversibly in normal water, eq 6, with k_D

$$KD \xrightarrow{k_D} E^- \underset{(+D^+)}{\overset{k_r}{\rightleftharpoons}} KH \quad (6)$$

$= k^{H_2O} + k^{OH}[OH^-]$. Loss of D^+ is rate determining provided subsequent proton equilibration is fast. Figure 3 shows that this is so under all pH conditions, and strictly first-order behavior was observed over at least the first 3 half-lives at each pH. Clearly k_0 may be equated with k_D. Melander and Saunders[14] have discussed similar situations in detail.

Table II compares rate constants for ^1H and ^2H transfer and gives primary isotope ratios for deprotonation by H_2O and OH^-. The latter values (k_H/k_D = 5.2 and 3.5, respectively) are in the range considered normal for carbon acid ionization. This aspect will be considered again below.

3. Buffer Catalysis in 1,3-Me$_2$-5-*t*-Bu(BA). Rate data for equilibration of the ^1H and ^2H forms of 1,3-Me$_2$-5-*t*-Bu(BA) in amine buffers are given in Table III (Supplementary Material). To reduce the relative importance of the solvolytic term (k_0) it was necessary in some cases to use higher buffer concentrations than those used for the solvolytic rate measurements. For $EtNH_2$, Et_2NH, and Et_3N with the ^1H substrate the k_0 contribution is appreciable even at 0.15 mol dm^{-3} (the highest concentration possible under our conditions). A similar situation obtains for NH_3 in the pH range 9.0–9.6, but dabco at pH 9.52 dominates the rate even at modest concentrations. High concentrations (up to 0.6 mol dm^{-3}) were necessary to define k^B accurately for 2,6-lutidine, particularly for the deuterated reactant.

Once the solvolytic contribution is subtracted from the observed rate ($k'_{obsd} = k_{obsd} - k_0$) the amine-catalyzed reaction of the ^1H reactant may be analyzed according to eq 7

$$KH + B \underset{k^{BH}}{\overset{k^B}{\rightleftharpoons}} E^- + BH^+ \quad (7)$$

where

$$k'_{obsd} = k^B[B] + k^{BH}[BH^+] \quad (8)$$

(14) Melander, L.; Saunders, W.H., Jr. *Reaction Rates of Isotopic Molecules*; Wiley: New York, 1980; p 287.

Table IV. Rate Constants for Base-Catalyzed Deprotonation and Dedeuteriation of 1,3-Dimethyl-5-*tert*-butylbarbituric Acid at 25 °C and I = 0.1 mol dm^{-3} (NaCl)

base	pK_{BH}	k_H^B (dm^3 mol^{-1} s^{-1})	k_D^B (dm^3 mol^{-1} s^{-1})	k_H/k_D
2,6-lutidine	6.77	0.0108	0.00106	10.0 ± 1.5
dabco	8.84	29.6	5.4	5.5 ± 0.5
NH_3	9.20	1.06	0.150	7.1 ± 1
$EtNH_2$	10.65	14.7	2.55	5.8 ± 0.6
Et_2NH	11.08	18.0	2.50	7.2 ± 0.8
Et_3N	10.78	1.30[b]	0.181[b]	7.2 ± 1.0
H_2O	−1.7	4.0×10^{-4}[a]	7.7×10^{-5}[a]	5.5[c]
OH^-	15.7	192	54	3.5[c,d]

[a] First-order rate constant (s^{-1}). [b] At I = 0.20 mol dm^{-3} (NaCl). [c] Ratio of computer fitted rate constants. [d] Comparison of k_{obsd} values using identical NaOH solutions gave a more precise value of this ratio (3.3 ± 0.3).

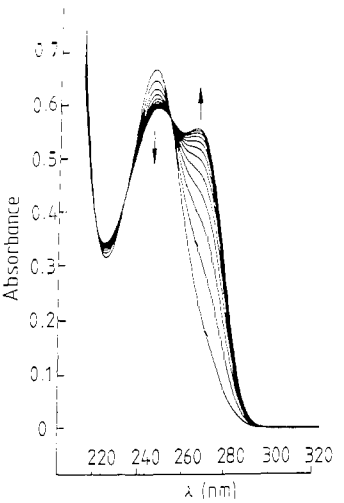

Figure 4. Spectral scans (interval 2 min) followed the addition of 5-*tert*-butylbarbituric acid (8.8×10^{-5} mol dm^{-3}, pH 3.0) to borax buffer (1.25×10^{-2} mol dm^{-3}, pH 9.8, 25 °C, I = 0.1 mol dm^{-3}).

Relating [KH] and [E$^-$] via K_c and [BH$^+$] and [B] via K_{BH}, the equilibrium condition (eq 9)

$$k^B[KH][B] = k^{BH}[E^-][BH^+] \quad (9)$$

becomes

$$k^{BH} = k^B\frac{K_{BH}}{K_c} \quad (10)$$

Substitution in 8 gives

$$k'_{obsd} = k^B[B]\left(1 + \frac{[H^+]}{K_c}\right) \quad (11)$$

For $[H^+] << K_c$ and $[H^+] >> K_c$ expression 11 reduces to $k'_{obsd} = k^B[B]$ and $k'_{obsd} = k^{BH}[BH^+]$, respectively. However, since the pH of the amine buffer was usually within 2 pH units of the substrate pK_c, the full expression 11, which allows for the contribution from reversibility, was used to evaluate k_H^B. These values are listed in Table IV.

For the ^2H reactant the k_D^B values (Table IV) were obtained from the relationship $k'_{obsd} = k_D^B[B]$. For the present series of reactions the reverse reprotonation step makes a negligible contribution to k_{obsd}, and the slope of k_{obsd} vs. [B] plots gives k_D^B.

4. CH and NH Acidity in 5-*t*-Bu(BA). When an acidic solution of 5-*t*-Bu(BA) (pH 3.0) (λ_{max} = 216 nm, $\epsilon = 7.4 \times 10^3$ dm^3 mol^{-1} cm^{-1}) is quickly adjusted to pH 9.8, the spectrum first observed (in the time of stopped-flow mixing, ≈ 3 ms) has λ_{max} = 248 nm, $\epsilon = 7.6 \times 10^3$ dm^3 mol^{-1} cm^{-1}, Figure 4. This spectrum then relaxes ($t_{1/2}$ = 247 s) to a final spectrum which possesses two maxima: one at 248 nm and the other at 267 nm. This process is also shown in Figure 4, and the rate of this reaction will be considered in detail in a following section. The final spectrum

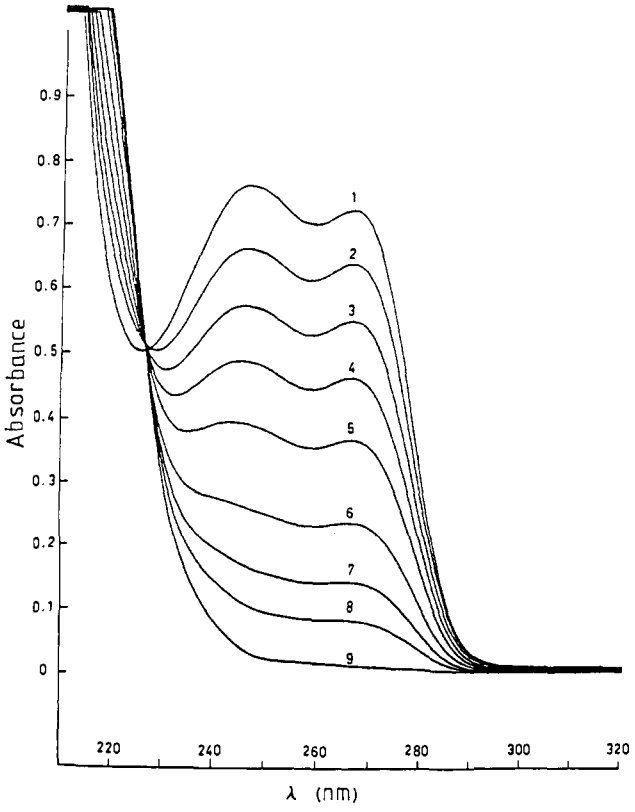

Figure 5. Spectrophotometric titration of 5-*tert*-butylbarbituric acid (1.15×10^{-4} mol dm^{-3}, $I = 0.1$ mol dm^{-3} NaCl) in the presence of hepes (1.0×10^{-3} mol dm^{-3}) at 25 °C with 0.1 mol dm^{-3} HCl. pH's: (1) 10.50; (2) 8.54; (3) 8.22; (4) 8.00; (5) 7.78; (6) 7.46; (7) 7.17; (8) 6.87; (9) 3.9.

remains unchanged on addition of further alkali up to pH 11, and reacidification (to pH 1–5) restores the initial 216-nm absorption. However, if the acidic (pH ~ 3) form of 5-*t*-Bu(BA) is directly adjusted to pH ~ 13.5 with NaOH, a different spectrum displaying a single absorption at 267 nm ($\epsilon = 5.8 \times 10^3$ dm^3 mol^{-1} cm^{-1}) is immediately observed. This change is also reversed on acidification.

The two reversible rapidly attained equilibria were investigated separately by pH perturbation methods by using spectral data taken within 10 ms of mixing. The species responsible for the 216- and 248-nm absorptions were linked (248-nm data) via a single ionization with $pK_{N_1} = 7.88 \pm 0.04$ at 25.0 °C and $I = 0.1$ mol dm^{-3} (NaCl). Similarly, the second ionization linking the 248- and 267-nm absorptions was investigated by rapid mixing to give final NaOH solutions of between 0.01 and 0.1 mol dm^{-3}. This data (248-nm) gave $pK_{N_2} = 12.4 \pm 0.1$.

If, however, sufficient time was allowed between successive pH adjustments such that the relaxation process referred to above was complete, a series of spectra were obtained (Figure 5) which gave $pK_a = 7.67 \pm 0.04$ at 25.0 °C and $I = 0.1$ mol dm^{-3} (NaCl) (248-nm data). This pK_a corresponds to a thermodynamic value of 7.89 which may be compared with a value of 7.96 determined potentiometrically.[15]

The above data are interpreted in terms of Scheme I. As a consequence of slow deprotonation at C_5 KH_2^- is the immediate product when solutions of KH_3 are made weakly basic ($pK_{N_1} = 7.88$), but following relaxation both the N and C deprotonated forms are present. Then

$$K_a = \frac{([KH_2^-] + [EH_2^-])[H^+]}{[KH_3]} = K_{N_1} + K_c \quad (12)$$

and the data give $K_c = (2.14 - 1.32) \times 10^{-8} = 8.2 \times 10^{-9}$ mol dm^{-3} ($pK_c = 8.09 \pm 0.12$). The $[KH_2^-]/[EH_2^-]$ ratio (K_1, Scheme I) of 1.6 ± 0.6 must clearly be pH independent.

(15) Wong, O. M. Pharm. Thesis, University of Otago, 1979.

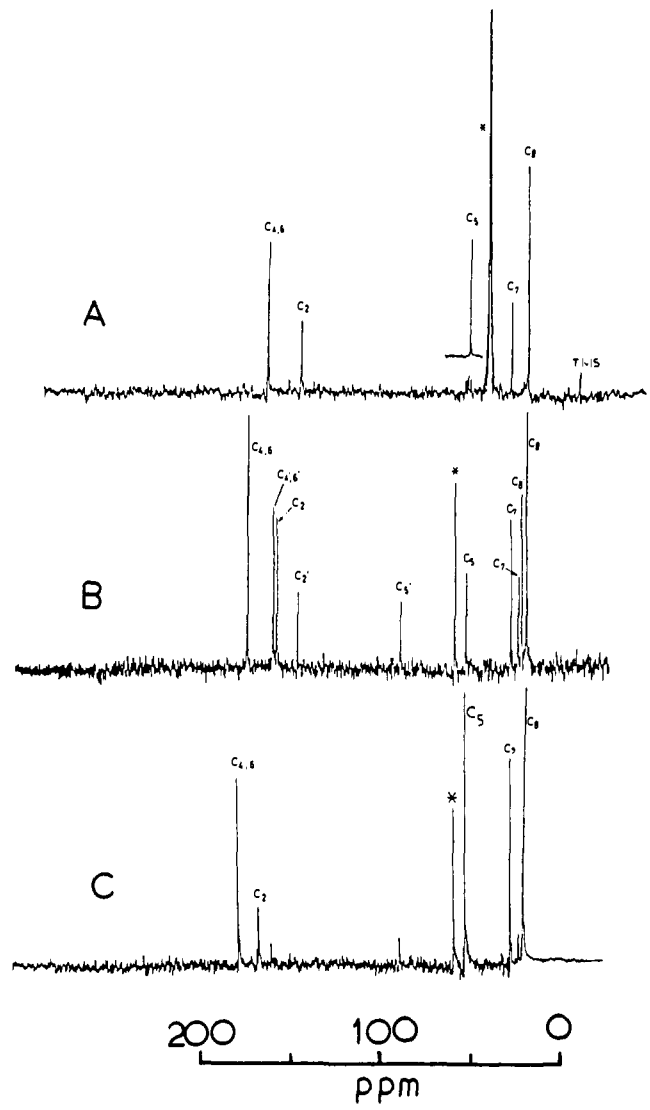

Figure 6. ^{13}C NMR spectra of 5-*tert*-butylbarbituric acid (184 mg): (A) in CH_3OD (C-5 in acetone-d_6), pulse width = 8 μs, delay = 20 s, no. of scans = 2883; (B) in 1.0 cm^3 H_2O and 0.50 cm^3 D_2O, 1 mol equiv of NaOH added, pulse width = 8 μs, delay = 10 s, no. of scans = 5816; carbon atoms denoted C_i' are assigned to EH_2^-; (C) in 1.0 cm^3 H_2O and 0.50 cm^3 D_2O, 2 mol equiv of NaOH added, pulse width = 8 μs, delay = 1 s, no. of scans = 9000. *CH_3OD signal in (A); dioxane reference in (B) and (C).

5. ^{13}C and ^1H NMR Spectra of 5-*t*-Bu(BA). The presence of distinct species which do not rapidly interconvert (on the NMR time scale) was clearly shown by ^{13}C and ^1H spectra on titrating with NaOH, and the number of such species is dependent on the amount of NaOH added. Figure 6A shows the proton decoupled ^{13}C NMR spectrum of 5-*t*-Bu(BA) in CH_3OD. Under these conditions the C_5 proton is largely deuterated, and decoupling leads

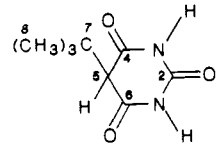

to loss of the C_5 signal. However, in $(CD_3)_2CO$ this problem is avoided, and C_5 appears at 60.75 ppm with the remaining carbons at similar chemical shifts to those found in CH_3OD. The assignments detailed in Table V (Supplementary Material) bear a close resemblance to those reported[16,17] for 5,5-Et_2(BA) (which

(16) Fratiello, A.; Mardirossian, M.; Chavez, E. J. *J. Magn. Reson.* **1973**, *12*, 221.

Scheme I

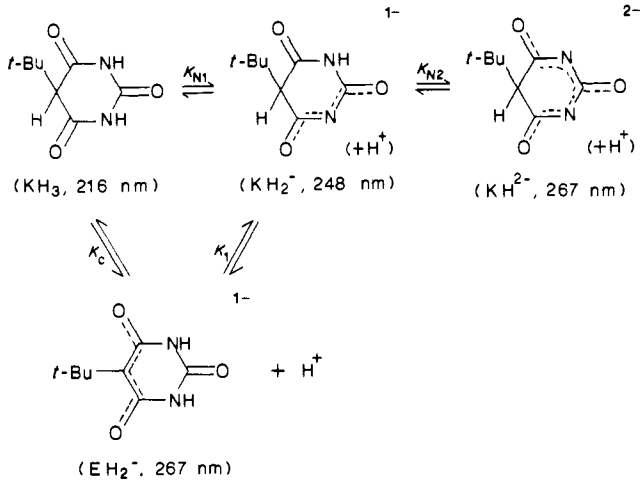

is known to crystallize in the ketonic form). On addition of 1 mol equiv of NaOH the barbituric acid is solubilized in H_2O, and 10 absorptions result, Figure 6B. These are assigned to KH_2^- and EH_2^-, present in a ratio of 1.75:1, by comparing the intensities of related signals. In this experiment delay times of 10 s between pulses was sufficient to allow all C atoms to relax, and the ratio is based on peak heights of C_8, C_8' and C_7, C_7' pairs. The chemical shifts of the *t*-Bu carbon atoms are little affected by NH ionization but are shifted slightly (C_7, +4 ppm; C_8, −3 ppm) by carbon ionization in EH_2^-. For similar reasons C_2' of EH_2^- is little affected, but C_2 of KH_2^- moves significantly downfield (ca. 13 ppm) consistent with ionization at the adjacent N centers. Ionization at C_5 causes $C_{4',6'}$ to move upfield (ca 4 ppm), while ionization at N results in a downfield shift (ca. 10 ppm). As expected C_5 is little affected by NH ionization but moves considerably downfield (ca. 37 ppm) when deprotonated. The ratio of 1.75 for $[KH_2^-]/[EH_2^-]$ (30 °C) agrees well with that found from UV spectra, 1.6 ± 0.6 (25 °C, I = 0.1 mol dm^{-3}).

Addition of a second mol equiv of NaOH causes the ten line spectrum to collapse to essentially a new five line spectrum, Figure 6C (traces of other species are also apparent). Although not appreciably hydrolyzed over the times necessary to collect this spectrum (16 h) appreciable degradation of the barbituric acid (to unknown products) was found after 48 h. The significant feature of Figure 6C is the position of C_5 (61.48 ppm) which differs little from that found for KH_3 (60.75 in acetone) and KH_2^- (61.64) and is appreciably upfield from that for EH_2^- (97.54). This implies that the species responsible is not ionized at C_5, i.e., is KH^{2-}, and that this is the major component present in strongly alkaline solution. Also to be noted is the fact that successive deprotonations at nitrogen (KH_3, KH_2^-, KH^{2-}) result in progressive shifts of C_2 and $C_{4,6}$ to lower fields; Table V (Supplementary Material) gives a listing of ^{13}C chemical shifts.

Figure 7 shows a series of 90-MHz ^1H spectra following successive additions of aqueous NaOH to 5-*t*-Bu(BA) in H_2O. After adding 1 mol equiv two *t*-Bu signals are observed consistent with the presence of both EH_2^- and KH_2^-. also the lower field signal (1.30 ppm) was observed to grow out of the higher field (1.03 ppm) signal so that the former may be assigned to EH_2^- and the latter to KH_2^-. Peak heights give $[KH_2^-]/[EH_2^-] \approx 2.0$ (32 °C). The C_5 proton can be observed at 2.87 ppm on the broad envelope of the H_2O resonance (peak height ratio 1:9 compared to 1.03 ppm signal). Further additions of NaOH show a gradual decrease in the 1.30 ppm signal with a corresponding growth in the 1.03 ppm resonance. After 2 equiv of NaOH are added, ca. 10% of the substrate is present as a distinct enolate species and after 4 mol equiv about 5%. However the 1.30 ppm signal does not completely disappear even after the addition of 6 mol equiv and the 1.03- and 2.87-ppm absorptions remain related by a peak height ratio of 9:1. The latter clearly corresponds to KH^{2-}, but the remaining 1.30 ppm resonance suggests the presence of small amounts of EH^{2-}. This is our only evidence for the existence of this species, and peak heights suggest a ratio $[KH^{2-}]/[EH^{2-}]$ of ≈ 20:1.

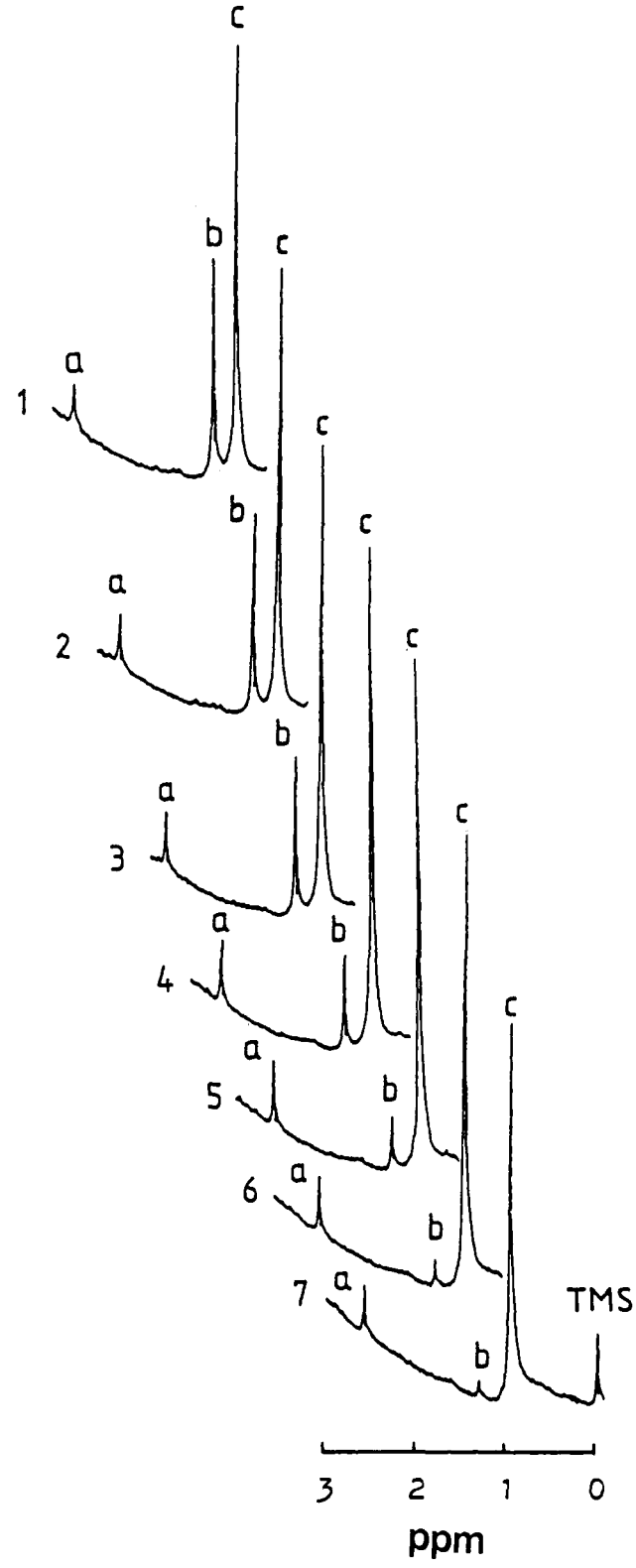

Figure 7. ^1H NMR spectra of 5-*tert*-butylbarbituric acid (36.8 mg, 2 × 10^{-3} mol) in H_2O (0.5 cm^3) following addition of NaOH solution (4 mol dm^{-3}). Mol equiv of NaOH added: (1) 1.0; (2) 1.25; (3) 1.5; (4) 2.0; (5) 2.5; (6) 4.0; (7) 6.0. Assignments: (a) C-5 $H(KH_2^-, KH^{2-})$; (b) *t*-Bu (EH_2^-, EH^{2-}); (c) *t*-Bu (KH_2^-, KH^{2-}).

6. ^1H and ^2H Transfer in 5-*t*-Bu(BA). ^1H exchange and ^2H transfer were studied over the pH range 6.5–13 by using the pH-jump method. Spectrophotometric rate data collected at 267

(17) Craven, B. M.; Vissini, E. A. *Acta Crystallogr. Sect. B: Struct. Cystallog. Cryst. Chem.* **1971**, *B27*, 1917.

Table VII. Rate Constants for Proton and Deuteron Transfer in 5-*tert*-Butylbarbituric Acid at 25 °C and I = 0.1 mol dm^{-3} (NaCl)

reactant	$k_1^{H_2O}$ (s^{-1})	k_1^{OH} (dm^3 mol^{-1} s^{-1})	k_2^{OH} (dm^3 mol^{-1} s^{-1})	k_{-1}^{H} (dm^3 mol^{-1} s^{-1})	$k_{-1}^{H_2O}$ (s^{-1})	$k_{-2}^{H_2O}K'_{N3}$ (dm^3 mol^{-1} s^{-1})
C-5 (^{1}H)	2.59×10^{-3}	800	0.543	3.2×10^5	1.62×10^{-3}	0.8
C-5 (^{2}H)	3.64×10^{-4}	234	0.043			
k_H/k_D	7.1	3.4	12.6			

Scheme II

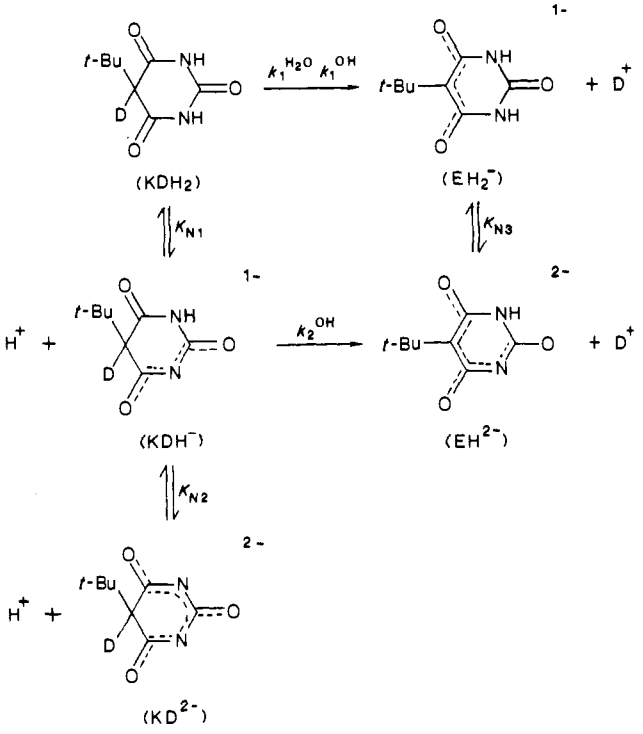

nm (Figure 4) are given in Table VI (Supplementary Material). Buffer catalysis (hepes, borax, Et_3N) was again observed, and plots of k_{obsd} vs. $[B]_T$ were linear. The extrapolated rate constants (k_0) at $[B]_T$ = 0 are also given in Table VI, and their variation with pH is shown in Figure 7.

Superficially these pH rate profiles resemble those found for 1,3-Me$_2$-5-*t*-Bu(BA) (Figure 3), but they do contain some important differences. These arise as a consequence of NH ionization which results in an increase in the number of pathways available for proton transfer to and from carbon. Such differences are seen, for example, as an absence of distinct minimum for the reaction of the ^{1}H substrate and in the departure from first order in [OH$^-$] kinetics for the ^{2}H derivative at high pH.

Because of this relative complexity, the kinetic analysis focused initially on the reaction of the ^{2}H compound where only the dedeuteriation rate (k_f) need be considered (c.f. eq 6). The k_0 data were analyzed according to Scheme II which allows paths for both H_2O- and OH$^-$-catalyzed dedeuteriation of KDH_2 and OH$^-$-catalyzed dedeuteriation of KDH$^-$ and where processes involving proton transfer to or from nitrogen or oxygen are assumed to be rapid (i.e., at equilibrium). This scheme leads to expression 13

$$k_0 = \frac{k_1^{H_2O}[H^+]^2 + k_1^{OH}K_w[H^+] + k_2^{OH}K_{N1}K_w}{[H^+]^2 + K_{N1}[H^+] + K_{N1}K_{N2}} \quad (13)$$

or its equivalent (eq 14)

$$k_0 = \frac{k_1^{H_2O} + k_1^{OH}[OH^-] + k_2^{OH}K_{N1}'[OH^-]^2}{1 + K_{N1}'[OH^-] + K_{N1}'K_{N2}'[OH^-]^2} \quad (14)$$

where $K_{N1}' = K_{N1}/K_w$, $K_{N2}' = K_{N2}/K_w$ ($K_w = K_w^T/f_+^2 = [H^+][OH^-] = 1.66 \times 10^{-14}$ mol^2 dm^{-6} at 25 °C and I = 0.1 mol dm^{-3}). Fitting the observed data to eq 14 was carried out by using the measured K_{N1} value for NH deprotonaion of the ^{1}H substrate

Scheme III

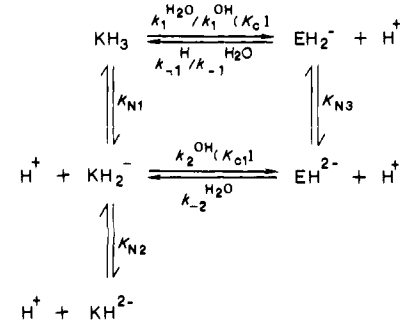

Scheme IV

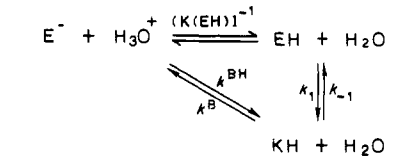

(1.32×10^{-8} mol dm^{-3}, $K_{N1}' = 8.0 \times 10^5$ dm^3 mol^{-1}). All other constants, including K_{N2}', were treated as variables. The results obtained, $k_1^{H_2O} = 3.64 \times 10^{-4}$ s^{-1}, $k_1^{OH} = 234$ dm^3 mol^{-1} s^{-1}, $k_2^{OH} = 4.3 \times 10^{-2}$ dm^3 mol^{-1} s^{-1}, and $K_{N2}' = 9.0$ dm^3 mol^{-1}, are represented by the full curve given in Figure 8. This K_{N2}' value gives pK_{N2} = 12.8 which may be compared with the value of 12.4 obtained by the spectrophotometric method for the protic substrate. The latter is likely to be the more reliable as the kinetic data does not extend beyond pH 12.9. Individual contributions by the three pathways as a function of pH are shown in Figure 9A. The H_2O ($k_1^{H_2O}$)- and OH$^-$ (k_1^{OH})-catalyzed dedeuteriation of KDH_2 dominates over the pH range 6.5–12, and the OH$^-$ pathway for KDH$^-$ (k_2^{OH}) only becomes significant above pH 11. However, this latter reaction dominates proceedings at pH 12.9 (90%).

The reaction of the ^{1}H substrate was analyzed in terms of Scheme III. Here each pathway for deprotonation necessarily corresponds to a similar pathway for dedeuteriation. Thus deprotonation follows eq 14, and since each pathway involving the basic reagents H_2O or OH$^-$ requires a reverse pathway for reprotonation by its conjugate acid, expression 15 holds for the

$$k_r = \frac{k_{-1}^{H}[H^+] + k_{-1}^{H_2O} + k_{-2}^{H_2O}K_{N3}'[OH^-]}{1 + K_{N3}'[OH^-]} \quad (15)$$

reverse reaction with $K_{N3}' = K_{N3}/K_w$. Since $K_{N3}'[OH^-] < 1$ (i.e., $K_{N3} < [H^+]$) over the pH range studied the observed rate, k_0, follows expression 16

$$k_0 = \frac{k_1^{H_2O} + k_1^{OH}[OH^-] + k_2^{OH}K_{N1}'[OH^-]^2}{1 + K_{N1}'[OH^-] + K_{N1}'K_{N2}'[OH^-]^2} + \frac{k_{-1}^{H}[H^+] + k_{-1}^{H_2O} + k_{-2}^{H_2O}K_{N3}'[OH^-]}{1 + K_{N1}'[OH^-] + K_{N1}'K_{N2}'[OH^-]^2} \quad (16)$$

The observed data were fitted to eq 16 by using the independently measured values of K_{N1}' (8.0×10^5 dm^3 mol^{-1}) and K_{N2}' (25 dm^3 mol^{-1}). Also, because of the identity relationships $k_1^{H_2O} = k_{-1}^{H}K_c$ and $k_1^{OH} = k_{-1}^{H_2O}K_c/K_w$; only one from each pair of rate constants was treated as an independent variable. In principle k_2^{OH} and $k_{-2}^{H_2O}$ could be similarly related via a knowledge of K_{N3}, but in the first instance k_2^{OH} and $k_{-2}^{H_2O}K_{N3}'$ were treated as independent variables in the fitting routine. The calculated curve given in Figure 8 was obtained by using the optimized values for $k_1^{H_2O}$, k_1^{OH}, k_2^{OH} and $k_{-2}^{H_2O}K_{N3}'$ given in Table VII. However,

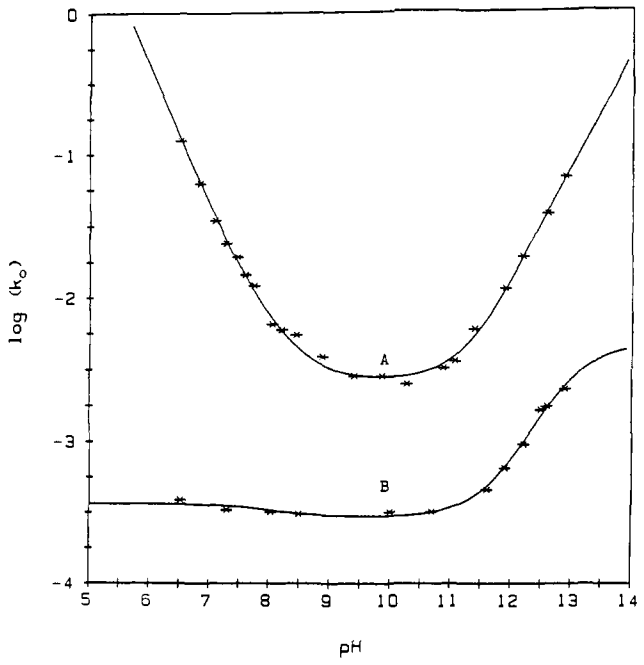

Figure 8. pH rate profiles for proton transfer (A) and dedeuteriation (B) at C_5 in 5-*tert*-butylbarbituric acid at 25 °C and I = 0.1 mol dm^{-3} (NaCl). Experimental points are indicated (*), and the curves are drawn by using eq 16 and 14, respectively, and the values of the constants given in the text and Table VII.

Scheme V

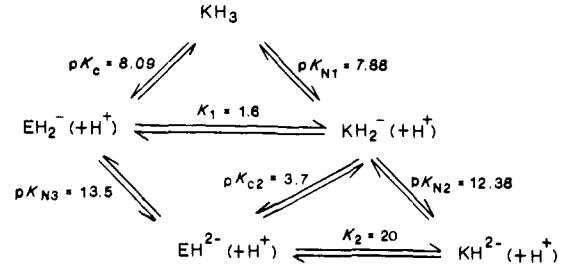

the ^{1}H NMR spectrum in strong alkali allows both K_{c1}(Scheme V) and K_{N3} to be estimated. Since this gave $[KH^{2-}]/[EH^{2-}] \approx 20$ then $K_{C1} \approx 2.1 \times 10^{-14}$ mol dm^{-3} ($pK_{c1} \approx 13.7$) and $K_{N3} \approx 3.4 \times 10^{-14}$ mol dm^{-3} (pK_{N3} = 13.5). Thus $k_{-2}^{H_2O} \approx 0.4$ s^{-1}.

Figure 9B shows the contributions made by the forward (k_f) and reverse (k_r) pathways for ^{1}H exchange. An interesting feature is the dominance of the observed rate (curve a) by the rate for reprotonation (curve b) over practically the entire pH range. At pH ~ 12 the forward rate (curve c) and reverse rate (curve b) assume equal importance, but at pH 13 the latter again dominates. The percentage contribution by each path is given in Figure 9C, and the dominance of the reverse paths k_{-1}^{H}, $k_{-1}^{H_2O}$, and $k_{-2}^{H_2O}K_{N3}'$ in particular pH regions is clearly evident.

Table VII also lists k_H/k_D ratios. For $k_1^{H_2O}$ and k_1^{OH} the values are comparable with those found for 1,3-Me_2-5-*t*-Bu(BA), Table II, but that for k_2^{OH} (k_H/k_D = 12.6) is unusually large. However, little significance can be attached to the latter result since the uncertainty in both k_2^{OH} rate constants is relatively high. The importance of the deuteron exchange study lay not in the determination of primary kinetic isotope effects but in the fact that it allowed the various pathways for proton exchange to be distinguished.

7. ^{1}H Exchange in 1,3-i-Pr_2(BA) and 1,5-*i*-Pr_2(BA). A limited kinetic study was carried out on these compounds at 25.0 °C and I = 0.1 mol dm^{-3} (NaCl). Measurements were made in acetate buffers, and the pH range (≈1 pH unit) was limited to regions where the reprotonation rate dominated k_{obsd} (pH < pK_c). Rate data are given in Table VIII (Supplementary Material) and correspond to values for reprotonation of the enolate anions (k^{H}_{-1})

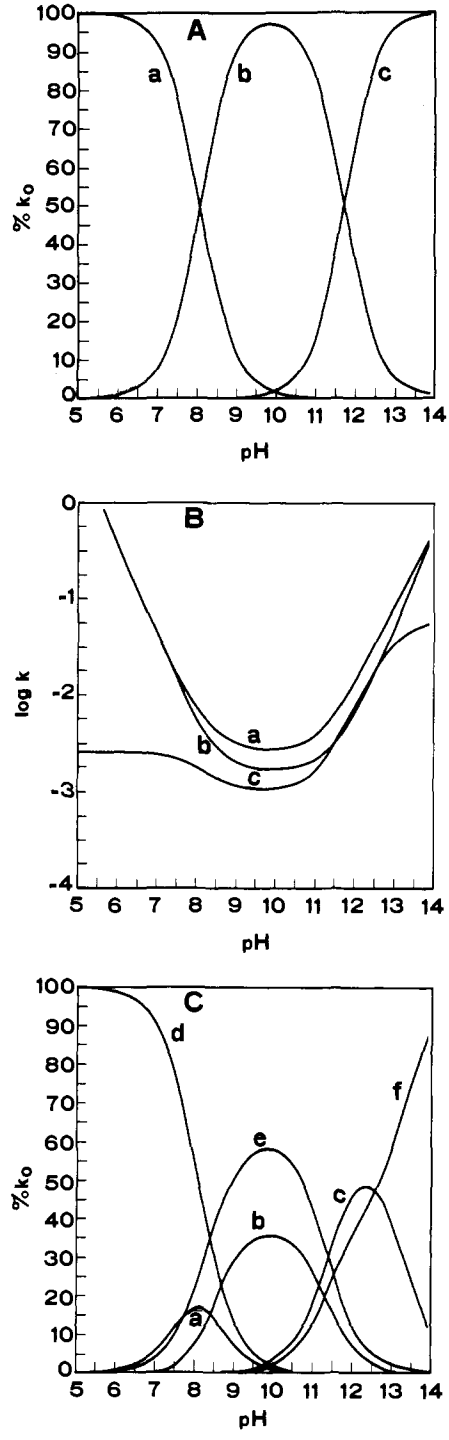

Figure 9. Proton and deuterium transfer in 5-*tert*-butylbarbituric acid at 25 °C and I = 0.1 (NaCl). (A) Percentage contribution to the observed dedeuteriation rates (k_0) of 5-*tert*-butylbarbituric acid from the $k_1^{H_2O}$ (a), k_1^{OH} (b), and k_2^{OH} (c) pathways at 25 °C. (B) Variation of log k with pH for proton transfer for (a) variation of log k_0 ($k_0 = k_f + k_r$), (b) variation of log k_r (reprotonation), and (c) variation of log k_f (deprotonation). (C) Percentage contribution to the observed proton transfer rates (k_0) to and from C_5. Contribution from $k_1^{H_2O}$ (a), k_1^{OH} (b), k_2^{OH} (c), k_{-1}^{H} (d), $k_{-1}^{H_2O}$ (e), and $k_{-2}^{H_2O}K'_{N3}$ (f).

of 1.17 × 10^6 dm^3 mol^{-1} s^{-1} (1,3-*i*-Pr_2(BA)) and 1.75 × 10^5 dm^3 mol^{-1} s^{-1} (1,5-i-Pr_2(BA)).

Discussion

Acidity Relationships. The assignment of the basic form of 1,3-Me_2-5-*t*-Bu(BA) to the enolate anion (E^-) appears unequivocal, but the acid form could exist as either the ketone (KH), the enol (EH), or as a mixture of the two. Several factors suggest that it is present as the ketonic form. (1) The slow spectral change

on titration with alkali (see below) is consistent with ionization at carbon but not oxygen. (2) The ratio ϵ_{max} (E^-)/ϵ_{max}(KH) of 2.3 agrees with similar ratios for other barbituric acids of known ketone structure.[18] For the ketonic forms the absorption maxima are dependent on substituents (e.g., λ_{max} = 212 nm for 5,5-Me_2(BA); λ_{max} = 227 nm for 1,3-Me_2(BA)), but the ϵ_{max} values are relatively insensitive, typically $\sim 10^4$ dm^3 mol^{-1} cm^{-1}. The absorption spectrum of the acid form of 1,3-Me_2-5-*t*-Bu(BA) is consistent with this (λ_{max} = 233 nm, ϵ = 7.1 × 10^3 dm^3 mol^{-1} cm^{-1}). (3) The ^{1}H NMR spectrum shows only one *t*-Bu signal in dilute DCl solution, but the limited solubility in acid would allow small amounts of EH to go undetected. (4) The agreement between the kinetic and spectrophotometric K_c values (3.55 × 10^{-10}, and 3.89 × 10^{-10} mol dm^{-3}, respectively) eliminates a significant EH contribution. If the latter were present, it would contribute to the spectrophotometric value but not to the kinetic value which must refer specifically to ionization at C_5. (5) Koffer[3] has shown that the EH:KH ratio for barbituric acids of differing acidity decreases markedly as ionization at carbon becomes more difficult. Thus p*K*(EH) varies little with substitution at C_5 (p*K*(EH) = 2.1–2.4) whereas pK_c(KH) is much more sensitive (p*K*(KH) = 2.2–4.9) with 55% EH occurring in 5-Ph(BA) (pK_c = 2.54) but only 0.3% in 5-*i*-Pr(BA) (pK_c = 4.91). Continuation of this trend to 1,3-Me_2-5-*t*-Bu(BA) (pK_c = 9.41) suggests the absence of EH for this very weak acid.

The acid–base equilibrium may then be represented as eq 17 with the negative charge of E^- residing largely on oxygen because of its greater electronegativity. Reprotonation by H_3O^+ (or BH^+)

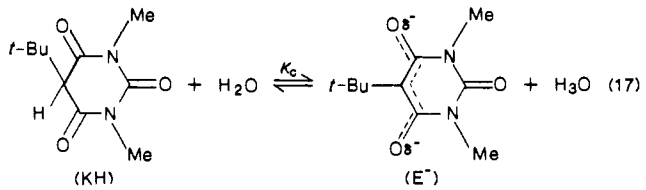

presumably occurs first at oxygen to form EH (diffusion controlled), but whether this is a kinetically viable intermediate which more slowly reverts to KH, or whether the process occurs directly via concerted reprotonation at C_5, Scheme IV, is not known. It was not possible to observe the spectrum of EH directly due to the rapidity of the H^+-catalyzed reprotonation reaction, but assuming the stepwise path and a p*K* for EH of 2.5 (suggested by the results of Koffer[3]) a specific rate for the EH–KH process (k_1, Scheme IV) of $\sim 3.6 \times 10^3$ s^{-1} may be calculated. However, it must be reemphasized that the details of proton abstraction and reprotonation at carbon are not determined by the present results. Jencks has considered analogous situations in some detail.[19]

Ionization in 5-*t*-Bu(BA) has been unravelled with the aid of UV spectral titration data, ^{13}C and ^{1}H NMR spectra, and kinetic studies. Scheme V gives a summary. Substitution of H by *t*-Bu at C_5 in barbituric acid decreases carbon acidity by 4.1 pK units and brings it into competition with ionization at the imide center. A similar decrease is more clearly observed for 1,3-Me_2(BA) (4.8 p*K* units) where imide ionization is absent.

N–H acidity is little influenced by *t*-Bu (or other alkyl) substitution at C_5. Successive ionizations at nitrogen of pK 7.88 and 12.38 (or 13.5 for EH_2^-) differ little from those for 5,5-Et_2(BA) (7.85, 12.5) or 1-Me(BA) (pK_{N2} = 12.8).[18] Generally for barbituric acids substitution at C_5 modifies, but does not alter, the normal pattern of initial ionization at C_5 to give EH_2^- (K_c) followed by ionization at N_1 or N_3 to give EH^{2-}. However, the present *t*-Bu acids are the least acidic barbituric carbon acids known, and this may arise in part from steric effects in EH_2^- where it is likely that the C_4–C_5–C_6 unit adopts a more planar conformation than in either KH_3 or KH_2^-. Such a situation occurs with 5-Et(BA) where crystal structures of both KH_3 and $K^+EH_2^- \cdot {}^5/_3H_2O$ are available.[20,21] For 5-*t*-Bu(BA) and 1,3-Me_2-5-*t*-Bu(BA) the bulky

Table IX. Rate Constants for Proton Abstraction ($k_1^{H_2O}$) and Enolate Reprotonation (k_{-1}^{H}) in Barbituric Acid (BA) and Its Derivatives at 25 °C[a]

compd	pK_c^T	$k_1^{H_2O}$ (s^{-1})	$10^{-5}k_{-1}^{H}$ (dm^3 mol^{-1} s^{-1})
1. 5-PhBA	2.20 (2.30)[d]	183	0.29[b]
2. BA	4.01 (4.05)[d]	26	2.63[b]
3. 5-MeBA	3.36 (3.58)[d]	24	0.56[b]
4. 5-EtBA	3.67 (3.80)[d]	16.9	0.79[b]
5. 5-*i*-PrBA	4.91 (4.94)[d]	1.32	1.07[b]
6. 1,3-*i*-Pr_2BA	5.65[e]	4.35	11.7[c]
7. 1,5-*i*-Pr_2BA	5.92[e]	0.349	1.75[c]
8. 5-*t*-BuBA	8.31[f]	0.0026	3.20[c]
9. 1,3-Me_2-5-*t*-BuBA	9.63[f] (9.60)[e]	0.0004	11.2[c]

[a] Data for entries 1–5 taken from ref 3. [b] $k_{-1}^{H} = k_1^{H_2O}/K_c^T$, ref 3. [c] $k_{-1}^{H} = k_1^{H_2O} f_\pm^2 / K_c^T$ ($f_\pm$ = 0.772, I = 0.1 mol dm^{-3} (NaCl)). [d] Potentiometric constant; McQueen, R. G. M. Pharm. Thesis, University of Otago, New Zealand, 1968. (*J. Chem. Soc. Perkin Trans. 2* **1974**, 1428). Determined under a nitrogen atmosphere by using solutions prepared from boiled out water distilled from $KMnO_4$ to avoid oxidation to 5-alkyldialuric acids (5-Me, -Et, -Ph). [e] Potentiometric constant, this work. [f] Spectrophotometric constant, this work.

t-Bu substituent probably presents an even larger barrier to the adoption of the planar conformation in the enolate anion through nonbonded interactions with the flanking carbonyl functions. However, attempts by us to obtain crystals of 5-*t*-Bu(BA) suitable for X-ray study as either KH_3 or its monoanions (KH_2^-, EH_2^- mixture as Na^+, K^+, Et_4N^+ salts) were not successful (only single thin needles or rosettes of needles were obtained from various water–alcohol–acetone mixtures). The demonstrated stabilization of KH_2^- over EH_2^- (K_1 = 1.6) and KH^{2-} over EH^{2-} ($K_2 \sim 20$), Scheme V, lends support to this argument; however, the alternative to destabilization of the EH_2^- ion would be to invoke some sort of solvent induced stabilization of the *t*-Bu keto acid KH_3 although why this might be so is less obvious. No evidence was found in this study for the trianion E^{3-}.

^{1}H Exchange and Rate–Acidity Relationships. A comparison of the rate constants given in Table II shows that OH^- is 3 × 10^7 more effective than H_2O in removing a proton from 1,3-Me_2-5-*t*-Bu(BA) whereas H^+ is 7 × 10^9 more effective than H_2O in reprotonating the enolate anion (these comparisons allow for the 55.5 mol dm^{-3} concentration of bulk water). Similar factors of 2 × 10^7 and 1.1 × 10^{10} hold for 5-*t*-Bu(BA), Table VII, although the rates are now ~ 5 and ~ 3 times faster than for its 1,3-dimethyl derivative. This accelerated rate may be due to steric factors arising from the presence of N-methyl substituents rather than from electronic factors. Removal of the proton from the anion KH_2^- by OH^- is understandably slower than deprotonation of KH_3 (k_2^{OH} = 0.54 dm^3 mol^{-1} s^{-1}, k_1^{OH} = 800 dm^3 mol^{-1} s^{-1}), but reprotonation of EH^{2-} by H_2O is not so retarded ($k_{-2}^{H_2O}$ = 0.4 s^{-1} vs. $k_{-1}^{H_2O}$ = 0.0016 s^{-1}).

Table IX lists all available data for the H_2O-catalyzed deprotonation and H^+-catalyzed reprotonation of barbituric acids. Unlike 5-*t*-Bu(BA) and 1,3-Me_2-5-*t*-Bu(BA), no additional data exists for the other barbituric acids for the OH^-/H_2O-catalyzed deprotonation/reprotonation processes,[3] although such pathways undoubtedly exist under alkaline conditions. Figure 10 gives Brønsted plots of log $k_1^{H_2O}$ and log k_{-1}^{H} against pK_c^T. The linear correlations have slopes α = 0.80 and β = 0.20, respectively. Thus for a $\sim 3 \times 10^7$ change in CH acidity $k_1^{H_2O}$ changes by a factor of 5 × 10^5 whereas k_{-1}^{H} changes by a factor of only 40. It is clear that substitution at C_5 affects the acid strength primarily through modification of the deprotonation rate. Similar observations have been made for keto acids and keto esters.[22] Pearson and Dillon[23] were the first to note such correlations in structurally related

(18) Fox, J. J.; Shugar, D. *Bull. Soc.* Chim. *Belges.* **1952**, *61*, 44.
(19) Jencks, W. P. *Chem. Soc. Rev.* **1981**, *10*, 345.
(20) Gatehouse, B. M.; Craven, B. M. *Acta. Crystallogr., Sect. B: Struct. Crystallogr. Cryst. Chem.* **1971**, *B27*, 1337.
(21) Gartland, G. L.; Gatehouse, B. M.; Craven, B. M. *Acta. Crystallogr., Sect. B: Struct. Cystallogr. Cryst. Chem.* **1975**, *B31*, 203.
(22) Bell, R. P. *The Proton in Chemistry*, 2nd ed.; Chapman and Hall: London, 1973; Figure 10, p 203.
(23) Pearson, R. G.; Dillon, R. L. *J. Am. Chem.* Soc. **1953**, *75*, 2439.

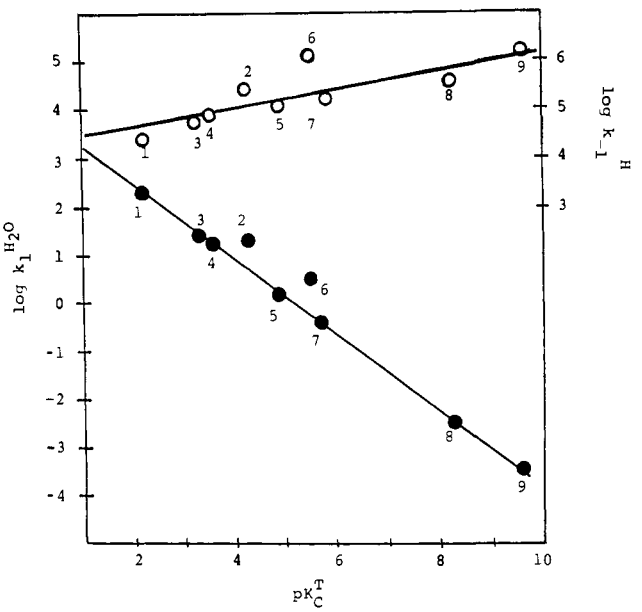

Figure 10. Dependence of the deprotonation rate constants ($k_1^{H_2O}$, ●) and recombination rate constants (k_{-1}^H, ○) on barbituric acid acidity at 25 °C: (1) 5-PhBA; (2) BA; (3) 5-MeBA; (4) 5-EtBA; (5) 5-*i*-PrBA; (6) 1,3-*i*-Pr_2BA; (7) 1,5-*i*-Pr_2BA; (8) 5-*t*-BuBA; (9) 1,3-Me_2-5-*t*-BuBA. pK_c^T and $k_1^{H_2O}$ for (2) and (6) are statistically corrected to allow for the presence of two hydrogens on C_5.

carbon acids, but for carbon acids of differing structure no relationship is apparent. Thus nitroethane is deprotonated some 10^6 times less rapidly than acetylacetone even though the two substrates have similar acidities ($pK_c \sim 9$).

The slowness of proton transfer in carbon acids can be directly attributed to the considerable electronic rearrangement involved in ionization. Some evidence for charge delocalization from carbon to oxygen in 5-*t*-Bu(BA) is found in the ^{13}C spectrum with $C_{4,6}$ moving upfield by ~4 ppm on deprotonation. Acids in which negative charge moves to a more electronegative atom as dissociation progresses have steeper energy profiles than normal oxygen or nitrogen acids and hence undergo slower proton transfers. Similarly, reprotonation by H^+ (k_{-1}^H) is also slower since the transition state now lies closer in energy to that of the enolate ion. Bell has discussed such situations by using potential energy diagrams.[24] Such observations imply that charge localization onto C is not well-advanced in the transition state for reprotonation (β small) and, conversely, that resonance development in the enolate ion lags behind C–H bond breaking in proton removal (α large). This agrees with the slopes depicted in Figure 10.

It is also apparent from Figure 10 that the rates of proton transfer to and from barbituric acids which do not have a C_5 substtuent (i.e., BA and 1,3-*i*-Pr_2(BA)) are anomalously high even after statistical correction (both K_C^T and $k_1^{H_2O}$ in Figure 10 have been corrected by a factor of 2). $k_1^{H_2O}$ and k_{-1}^H are 2–5 times larger than expected. Such deviations could arise from a reduction in electronic or rehybridization effects in the H-substituted C_5 anion compared to the R-substituted anion. This would imply a greater degree of carbanion character in the former with less electron delocalization to oxygen. It is less likely that the deviations could arise from steric factors unless these are specific to the R = H acid.

General Base Catalysis and Primary Kinetic Isotope Effects. Comparisons of k_H^B (or k_D^B) data with K_{BH} (Table IV) shows that there is no Brønsted relationship of the form $\log k_H^B = \beta pK_{BH} + C$ between the rate constant for proton abstraction from 1,3-Me_2-5-*t*-Bu(BA) and the acidity of the abstracting base. Even for the series of amine bases NH_3, $EtNH_2$, Et_2NH, and Et_3N there is little correspondence with amine basicity. Thus, while $EtNH_2$ is a somewhat weaker base than Et_3N it is 11 times more effective in proton abstraction, while dabco is some 20 times more effective than Et_3N although it is some 10^2 times less basic. Clearly structural effects play an important role with accessibility to the C_5 center probably being important. The least hindered bases, and those with tied back substituents such as dabco, are most effective. Although well-known in O and N acid chemistry such structural effects are less well documented for C acids.[25]

The bulky *t*-Bu group adjacent to the proton undergoing transfer must also play a role, and we decided to look at the primary kinetic isotope effect of replacing ^1H by ^2H to see if unusually large k_H/k_D ratios were involved. Previous investigations in this area have centered principally on reactions involving steric hinderance in the abstracting base rather than in the carbon acid. With 1,3-Me_2-5-*t*-Bu(BA) there is the possibility of having large steric factors present in both acid and base.

Values of k_H/k_D greater than 12 are considered abnormally high and not explicable in terms of the absolute reaction rate theory. Melander and Saunders[26] cite 15 reactions giving large isotope effects, and the majority involve proton abstraction from a nitroalkane by a hindered pyridine. While most values fall in the range 12–16, there are three (24.8, 19.5 and 27) which stand apart; these are believed to arise as a consequence of quantum mechanical tunnelling. All three reactions involve deprotonation by the highly hindered base 2,4,6-collidine (the first value has since been amended to 16).[27] Steric effects are believed to cause a steep rise in potential energy upon close approach of the reactants, and the resulting high and narrow barrier favors transfer of the lighter isotope. However, McLennan has successfully modelled such large isotope ratios via loose transition states without the aid of quantum mechanical tunnelling.[28]

1,3-Me_2-5-*t*-Bu(BA) provides an entirely different C-acid without an (activating) NO_2 substituent but which, because of its steric properties, was considered a likely candidate for an unusually large hydrogen primary isotope effect. Inspection of Table IV, however, shows that this expectation is not realized with proton abstraction by OH^-, H_2O, Et_2NH, $EtNH_2$, NH_3, Et_3N, and dabco giving k_H/k_D values which are essentially in the normal range. Only with 2,6-lutidine was an appreciably larger isotope effect observed ($k_H/k_D = 10 \pm 1.5$), and this is still explicable if C–H bending modes are weakened in the transition state, i.e., there is no need to invoke quantum mechanical tunnelling. 2,6-Lutidine provides the greatest steric barrier to reaction of any of the bases studied, but it is worth noting that as the steric barrier to reaction increases the difficulty in measuring precise general base-catalyzed rates in water as solvent is also increased. This is due to the large contribution to k_{obsd} by the OH^--dependent term (k^1_{OH}). Because of this problem it is difficult to see how the use of even more hindered bases, which might provide larger k_H/k_D ratios, could provide meaningful results. Also, the observed ~10^7 difference between $k^1_{H_2O}$ and k^1_{OH} found here (Table IV) means that only minor differences in their relative contributions to the rate (rather than in their magnitude) for the ^1H and ^2H substrates is necessary to cause a rather large variation in the apparent isotope ratio (a factor of 2 results from this cause with 5-*t*-Bu(BA)). Because of these difficulties it appears to us that in some of the cases quoted by Melander and Saunders, where large k_H/k_D ratios are reported for proton transfer to hindered bases, the solvent contribution to the observed rates has not been adequately explored.[29,30]

Registry No. 1,3-Me_2-5-*t*-BuBA, 7435-62-3; 5-*t*-BuBA, 90197-63-0; 1,3-*i*-Pr_2BA, 66400-12-2; 1,5-*i*-Pr_2BA, 7770-84-5; D_2, 7782-39-0.

(24) Reference 22, Figure 14, p 209.

(25) Kresge, A. J. In *Proton Transfer Reactions*; Caldin, E. F.; Gold, V., Eds.; Chapman and Hall: 1975; p 179.
(26) Reference 14, Table 5.1, p 142.
(27) Isaacs, N. S.; Javaid, K. *J. Chem. Soc., Perkin Trans. 2* **1979**, 1583.
(28) McLennan, D. J. *Aust. J. Chem.* **1979**, *32*, 1883.
(29) O'Ferrall, R. A. M. in ref 25, p 201.
(30) Bernasconi, C. F. *Pure Appl. Chem.* **1982**, *54*, 2335.

Supplementary Material Available: Rate data for proton and deuteron transfer (Table I) and amine-catalyzed deprotonation and dedeuteriation (Table III) of 1,3-Me_2-5-*t*-Bu(BA) for proton and deuteron transfer in 5-*t*-Bu(BA) (Table VI) and for proton transfer in 1,3-*i*-Pr_2(BA) and 1,5-*i*-Pr_2(BA) (Table VIII) are available as are ^{13}C chemical shifts in 5-*t*-Bu(BA) (Table V) (12 pages). Ordering information is given on any current masthead page.

The Crystal and Molecular Structure of Tris(substituted amino) Sulfonium Ions

William B. Farnham,* David A. Dixon,* William J. Middleton, Joseph C. Calabrese, Richard L. Harlow, J. F. Whitney, Glover A. Jones, and Lloyd J. Guggenberger

Contribution No. 4038 from the Central Research and Development Department, E. I. du Pont de Nemours and Company, Inc., Experimental Station, Wilmington, Delaware 19898. *Received May 14, 1986*

Abstract: The synthesis and crystal structures determined by X-ray diffraction techniques for a number of salts of the tris(dimethylamino)sulfonium cation (methyl-TAS) are reported. The structures of the methyl-TAS cation are all very similar, and the cation possesses approximate C_s symmetry with two equivalent $(CH_3)_2N''$ groups and one unique $(CH_3)_2N'$ group. The structure is characterized by a long S–N′ bond distance of 1.689 Å and two short S–N″ bond distances of 1.615 Å. The N″–S–N″ bond angle is large, 115.4°, while the two N′–S–N″ bond angles are smaller, 99.2°, similar to those in other sulfonium ions. The unique amino group is pyramidal, and the equivalent amino groups are approximately planar. The results suggest multibonding character in the S–N″ bonds. Ab initio molecular orbital calculations on $S(NH_2)_3^+$ with a large basis set confirm the observed X-ray crystal structure. A detailed conformational analysis of the surface for inversion at S^+ is presented. Analytically calculated infrared frequencies and intensities are presented, and these results are consistent with the observed structures. The sulfur is found to be quite positive, $q(S) = 0.92e$. The crystal structure of a tricyclic TAS derivative is also presented. Ring strain causes deviations from the preferred structure found for methyl-TAS. A very short nominally nonbonded S–O distance of 2.55 Å is observed.

Tris(dialkylamino)sulfonium cations, $(R_2N)_3S^+$,[1] are unique in their ability to form stable, isolable salts containing a variety of unusual anions. Among these anions are difluorotrialkylsiliconates,[2] perfluorinated alkoxides,[3] perfluorinated carbanions,[4] and hypervalent iodinanides.[5] The convenient chemical and physical properties of several of these species have led to structural determinations, studies of dynamic properties in solution, and a variety of new synthetic methods.[6] TAS salts were also important in early studies which led to the group transfer polymerization process.[7]

We have characterized the structures of six tris(dimethylamino)sulfonium (methyl-TAS) salts: methyl-TAS + I^- (**1**), methyl-TAS + Br^- (**2**), methyl-TAS + FHF^- (**3**), methyl-TAS + CF_3O^- (**4**), methyl-TAS + 5′ (**5**), and methyl-TAS + 6′ (**6**).

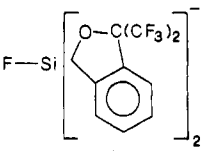

5′

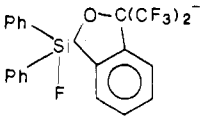

6′

The structure of the salt **8** of 5′ with another TAS derivative **7**, has also been studied. The structures of **4**[3] and **5**[8] have been reported by us previously with the focus on the structures of the anions.

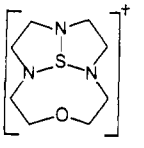

7

We have also calculated the structure of $(R_2N)_3S^+$ for R = H (**9**) by using ab initio molecular orbital theory with a large basis set. The calculations provide more information about the electronic structure and conformational properties of this novel ion and provide insight into the ion's unusual bonding.

Experimental Section

Synthesis. General Remarks. Proton and fluorine chemical shifts are reported in ppm downfield from tetramethylsilane and $CFCl_3$, respectively. ^1H NMR spectra were recorded on a Nicolet NT WB-360

(1) We have chosen the acronym TAS (tris amino sulfonium) to represent this class of cations.

(2) (a) Middleton, W. J. U.S. Patent 3 940 402, Feb 1976. (b) Middleton, W. J. *Org. Synth.* **1985**, *64*, 221.

(3) Farnham, W. B.; Smart, B. E.; Middleton, W. J.; Calabrese, J. C.; Dixon, D. A. *J. Am. Chem. Soc.* **1985**, *107*, 4565.

(4) (a) Smart, B. E.; Middleton, W. J.; Farnham, W. B. *J. Am. Chem. Soc.* **1986**, *108*, 4905. (b) Farnham, W. B.; Middleton, W. J.; Fultz, W. C.; Smart, B. E. *J. Am. Chem. Soc.* **1986**, *108*, 3125.

(5) Farnham, W. B.; Calabrese, J. C. *J. Am. Chem. Soc.* **1986**, *108*, 2449.

(6) Much of the synthetic work features TAS difluorotrialkylsiliconates as potent, anhydrous sources of fluoride. See, for example: (a) Noyori, R.; Nishida, I.; Sakata, J. *Tetrahedron Lett.* **1980**, 2085. (b) Noyori, R.; Nishida, I.; Sakata, J.; Nishizawa, M. *J. Am. Chem. Soc.* **1980**, *102*, 1223. (c) Noyori, R.; Nishida, I.; Sakata, J. *J. Am. Chem. Soc.* **1981**, *103*, 2108. (d) RajanBabu, T. V. *J. Org. Chem.* **1984**, *49*, 2083. (e) RajanBabu, T. V.; Fukunaga, T. *J. Org. Chem.* **1984**, *49*, 4571. (f) RajanBabu, T. V.; Reddy, G. S.; Fukunaga, T. *J. Am. Chem. Soc.* **1985**, *107*, 5473. (g) Fujita, M.; Hiyama, T. *J. Am. Chem. Soc.* **1985**, *107*, 4085. (h) Card, P. J.; Hitz, W. D. *J. Am. Chem. Soc.* **1984**, *106*, 5348. (i) Trainor, G. C. *J. Carbohydr. Chem.* **1985**, *4*, 545. (j) Fujita, M.; Hiyama, T. *J. Am. Chem. Soc.* **1985**, *107*, 8294.

(7) Webster, O. W.; Hertler, W. R.; Sogah, D. Y.; Farnham, W. B.; RajanBabu, T. V. *J. Am. Chem. Soc.* **1983**, *105*, 5706. Webster, O. W. U.S. Patent 4 417 034, Nov 1983.

(8) Farnham, W. B.; Harlow, R. L. *J. Am. Chem. Soc.* **1981**, *103*, 4608.

0002-7863/87/1509-0476$01.50/0